Metallography, Microstructure, and Analysis
https://doi.org/10.1007/s13632-024-01047-4

ORIGINAL RESEARCH ARTICLE

Effect of Rare Earth Elements Addition and Sintering Conditions on the Microstructure and Microhardness of Inconel 718

H. M. Medrano-Prieto[1] · A. Santos-Beltrán[1] · V. Gallegos-Orozco[1] · M. M. Santos-Beltrán[1] · H. Camacho-Montes[2] · C. G. Garay-Reyes[3] · M. A. Ruiz-Esparza-Rodriguez[3] · I. Estrada-Guel[3] · G. Rodríguez-Cabriales[3] · J. C. Guía-Tello[4] · J. M. Mendoza-Duarte[3] · J. M. Silva-Aceves[2] · J. S. Castro-Carmona[2] · R. Martínez-Sánchez[3,5]

Received: 19 October 2023 / Revised: 9 January 2024 / Accepted: 15 January 2024

Abstract

A series of Inconel 718 alloys modified by additions of 0.1-0.3 of a mixture of rare earth elements Ce:La:Nd:Pr have been synthesized by powder metallurgy. These alloys were sintered by conventional and hot isostatic pressure methods and subject to standard aging treatment. The results showed that adding rare earth elements generates γ′ and γ″ precipitates with a minor size than those reported. Additionally, the presence of rare earth elements causes the formation of La-Ti-Al-O phases that act as reinforcing particles. The highest microhardness values were obtained in the samples with 0.3 wt.% of rare earth elements and sintered by hot isostatic pressure. These hardness values are attributed to the precipitation of the nanophases (γ′ and γ″), the high numeric density of dispersed oxides and carbides, and solid solution strengthening generated by rare earth elements addition and dissolution of elements in the Nb, Ti and Mo rich phases.

Keywords Rare earth element · Hot isostatic pressing · Microstructure · Vickers microhardness test · Inconel 718

Introduction

The Nickel-base Superalloy Inconel 718 (IN718) has excellent properties for high-temperature applications, such as aeronautic and aerospace engines, nuclear power generation and petrochemical industries [1–3] due to its high resistance to oxidation and good mechanical properties at elevated work temperatures. In this sense, the Powder Metallurgy (PM) and the Hot Isostatic Pressing (HIP) processes have produced parts with excellent mechanical properties due to the retention of both refined microstructure and high homogeneity provided by PM, combined with the high densification reached by HIP [4, 5]. Additionally, heat treatments are used to enhance mechanical performance due to the precipitation of phases such as the γ′-Ni_3(Al, Ti) and the γ″-Ni_3Nb during aging heat treatments [4–8].

In the last 20 years, significant advances have been made in the effect of Rare Earth Elements (REE) additions on the properties of superalloys. The use of Re, Hf, Ta, Nb, and Ru, among others, has increased due to the need to obtain superalloys with attractive mechanical properties superior to the current ones. For example, it has been reported that Y and Ce additions have positive effects on the solid solution hardening, which is due to an increment in the lattice mismatch, as well as in the grain boundary cohesion, modification of carbides and eutectic phases morphology; which significantly improves the mechanical properties of superalloys at elevated temperatures [9–11].

✉ C. G. Garay-Reyes
carlos.garay@cimav.edu.mx

✉ R. Martínez-Sánchez
rmtzschz@gmail.com

1 Departamento de Nanotecnología, Universidad Tecnológica de Chihuahua Sur, Km. 3.5 Carr. Chihuahua a Aldama, 31313 Chihuahua, Chihuahua, Mexico

2 Universidad Autónoma de Ciudad Juárez (UACJ), Av. Plutarco Elías Calles No1210 Fovissste Chamizal, 32310 Ciudad Juárez, Chihuahua, Mexico

3 Centro de Investigación en Materiales Avanzados (CIMAV), Miguel de Cervantes No. 120, 31136 Chihuahua, Chihuahua, Mexico

4 Departamento de Metal-Mecánica, Tecnológico Nacional de México/IT de Saltillo, Venustiano Carranza 2400, Tecnológico, 25280 Saltillo, Coahuila, Mexico

5 Instituto de Metalurgia, Universidad Autónoma de San Luis Potosí, Sierra Leona No. 550, 78210 San Luis Potosí, Mexico

Published online: 13 February 2024

In this sense, this research is related to previous investigations that have studied the effect of oxide dispersion and alloying element additions in Ni-base superalloys produced by the Mechanical Alloying Process (MA). Li Yu et al. [12] have studied the oxide dispersion and Al/Ti atomic ratio on microstructural and hardness properties in Ni-base superalloys; they reported a strengthening effect in alloys with high Al/Ti atomic ratio attributed to nanoscale oxides. Seyyed Aghamiri et al. [13] studied the influence of MA and the Y-Hf additions on oxide dispersion strengthened Ni-base superalloys; they reported that morphological changes in γ′ phase decrease the elastic strain energy of the precipitates and Hf addition promoted the refinement of precipitated oxide particles in γ phase. Other research works [4, 5] have studied the effects of HIP, the standard heat treatment and solution heat treatment temperature in IN718 fabricated by PM. The results showed essential increments in mechanical properties with competent elongation levels due to the dissolution of carbides, precipitation of γ′ and γ″ phases during heat treatments and a fine-grain microstructure. Moreover, the use of REE and a sintering process provided by HIP has not been deeply investigated in IN718 alloy. However, the REE additions and HIP sintering process are potential modifications to improve superalloys' mechanical and microstructural properties.

Experimental Procedure

The IN718 alloy and those modified with REE additions were synthesized by the MA process. An IN718 commercial alloy was employed as raw; the use of a mixture of REE based on previous results [14, 15], is a commercial mischmetal (rare earth alloy composed with a higher content of lanthanum and cerium) with a purity of 99 % and content of Ce:La:Nd:Pr: 50-55:30-35:5-10:5-10: (wt.%). Modified alloys with 0.1, 0.2 and 0.3 of REE (wt.%) were obtained by MA in a high-energy mill Spex 8000. The milling process was done for 5 h in a hardened steel vial with hardened steel balls as milling media. All milling runs were performed with N-heptane as the process control agent, and Ar gas was used as an inert milling atmosphere using a ball-to-powder ratio of 5:1 to obtain 8.5 g of alloyed powder. The powder's compaction was done using a hydraulic press and a compaction pressure of 1.56 GPa for 5 min. The Conventional Sintering Process (CS) was carried out at 1200 °C for 4 h in vacuum-sealed quartz ampoules. The HIP process was performed at 1200 °C for 4 h at 120 MPa under an Ar atmosphere. Standard heat treatment was carried out for both sintering conditions: Solution heat treatment at 980 °C for 1 h and quenched in water at room temperature and two-step aging treatment, heating at 720 °C for 8 h, cooldown rate of 55 °C/h until 620 °C and hold for 8 h before air cooling to room temperature. The structural and microstructural characterization was carried out by a Panalytical X'Pert PRO x-ray diffractometer (XRD), Scanning Electron Microscopes (SEM) HITACHI SU3500 and FE-SEM JSM-7401F, Transmission Electron Microscopes (TEM) JEOL TM JEM2200F + CS operated at 200 kV and HITACHI 7700 operated at 100 kV. SEM samples were prepared following standard metallographic techniques. TEM samples were prepared using a Focused Ion Beam (FIB) model JEM-9320FIB with an Omniprobe 200 nanomanipulator. The Vickers Microhardness (HV) was evaluated in the LM300 AT tester with 100 g of load and 15 s of dwell time. The indentations were done in different sample locations following the standard ASTM designation E92. Quantification of hardness was based on analysis of at least 6 indentations.

Results and diskussion

Figures 1 and 2 show SEM-COMPO micrographs of microstructure in IN718 alloy and the alloy with 0.3 REE (wt.%) after HIP sintering and aging treatment and Energy Dispersive Spectroscopy (EDS)-mapping and chemical composition of principal phases in IN718 aged alloy with 0.3 REE (wt.%) after CS (c) and HIP (d) sintering. The microstructures present irregular morphology phases

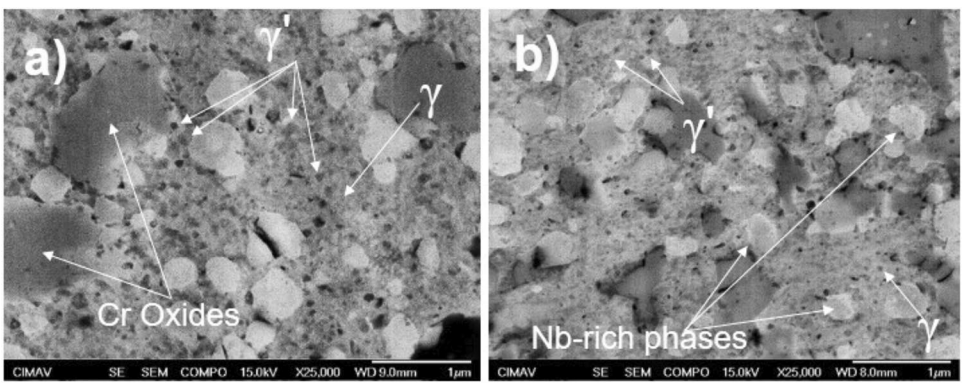

Fig. 1 SEM-COMPO micrographs corresponding to the microstructure of the IN718 alloy (**a**) and alloy with 0.3 REE (wt.%) (**b**) after HIP sintering and aging treatment.

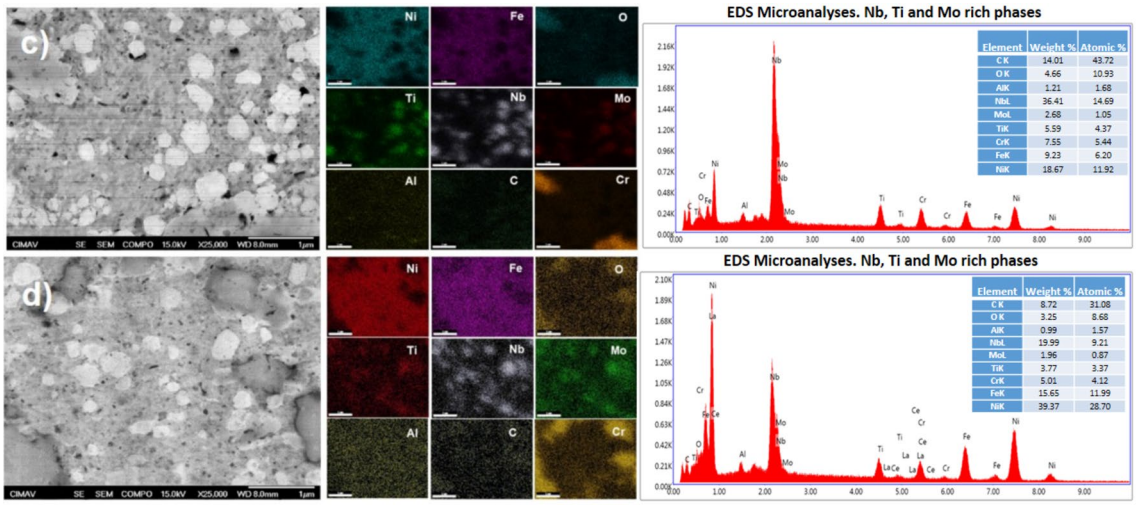

Fig. 2 EDS-mapping of the IN718 aged alloy with 0.3 REE (wt.%) after conventional (**c**) and HIP (**d**) sintering.

(dark gray), rounded morphology phases (white), and γ′ precipitate phases in the modified and unmodified IN718. According to the EDS-mapping, the rounded morphological phases (white) correspond to Nb, Ti and Mo-rich phases. The irregular morphology phases (dark gray) correspond to Cr oxides, and the γ matrix phase is Ni, Fe, Cr and Mo rich. The microstructure observed is in accord with the results of Appa Rao et al. [4, 5], who reported a homogeneous microstructure integrated for a solid solution of NiFeCrMo (γ matrix), acicular and rounded morphology phases that correspond mainly to oxides, blocky type carbides, which are Nb-Ti enriched and the presence of δ-precipitates (Ni_3Nb) with acicular morphology. When comparing the CS and HIP sintering, a minor concentration of the elements Nb, Ti and Mo (white) are observed in HIP sintering; such behavior could be attributed to the slow cooling rate provided by HIP. This slow cooling favored a greater diffusion of Nb-rich phases toward the γ matrix than CS sintering.

Figure 3 shows the XRD patterns corresponding to IN718 alloy and alloy with 0.3 REE (wt%) after CS and HIP sintering and aging treatment. In both sintering processes, the main peaks observed in the alloys were identified as γ matrix and Nb-Ti enriched carbide. This carbide, which presents a dissolution temperature of ≈1176 °C, was expected due to the solution treatment temperature of 980 °C [6]. Peaks corresponding to REE and δ phase were not observed, owing to the low REE concentration and the diffractometer's detection limit.

Figure 4 shows a Scanning Transmission Electron Microscopy Bright Field (STEM-BF) micrographs and their corresponding EDS-mapping of IN718 alloy with 0.3 REE (wt.%) after HIP sintering and aging treatment. The results reveal that one of the rounded morphology phases with a size of 105 nm is composed mainly of Al and O, previously reported in this alloy system [4, 16]. The affinity of La with Ti, Al, and O is observed in another phase with a size of 125 nm (red square). In addition, the presence of Cr and O-rich phases, which possibly correspond to Cr_2O_3 [6], and the homogeneous distribution of Nb and Ce elements is observed.

Figure 5 shows a TEM-BF micrograph and the NanoBeam Electron Diffraction (NBED) pattern corresponding to the IN718 alloy with 0.3 RE (wt.%) after HIP sintering and aging treatment. Precipitates uniformly distributed in the γ matrix can be noticed with disk-shaped morphology and aligned along < 100 > direction. According to previous research, these phases correspond to γ″ (Ni_3Nb) precipitates which have been reported with Body-Centered Tetragonal (BCT) structure, lattice parameters a = 0.361 nm, c = 0.743 nm, space group I4/mmm [4, 5, 7, 8], and orientation relationship {100} γ″//{100} γ and [001] γ″// < 100 > γ [7]. Previous studies [7] have reported that γ″ precipitates in IN718 alloy possess a length from 10 nm and 30 nm after 4 h of aging treatment at 680 °C and 750 °C, respectively [7]. These authors have reported that γ″ precipitates are fully coherent with γmatrix when its length < 30 nm. On the other hand, quasi-spherical precipitates corresponding to γ′ Ni3(Ti, Al) phase are observed. Investigations have reported γ′ precipitates with a diameter from 6 to 33 nm in different periods of aging treatment at temperatures between 680 and 750 °C [7]. These precipitates have been reported to be fully coherent with the γ matrix and present a Face Cubic Centered (FCC) structure [4, 5, 7]. Also, γ′ precipitates with a cuboidal-shaped morphology are observed. Nevertheless, this morphology is more frequently observed in Ni-base superalloys with low Fe content [2]. The micrograph shows a lower number density of γ′ precipitates concerning γ″, and this behavior is in accord with previous results of other

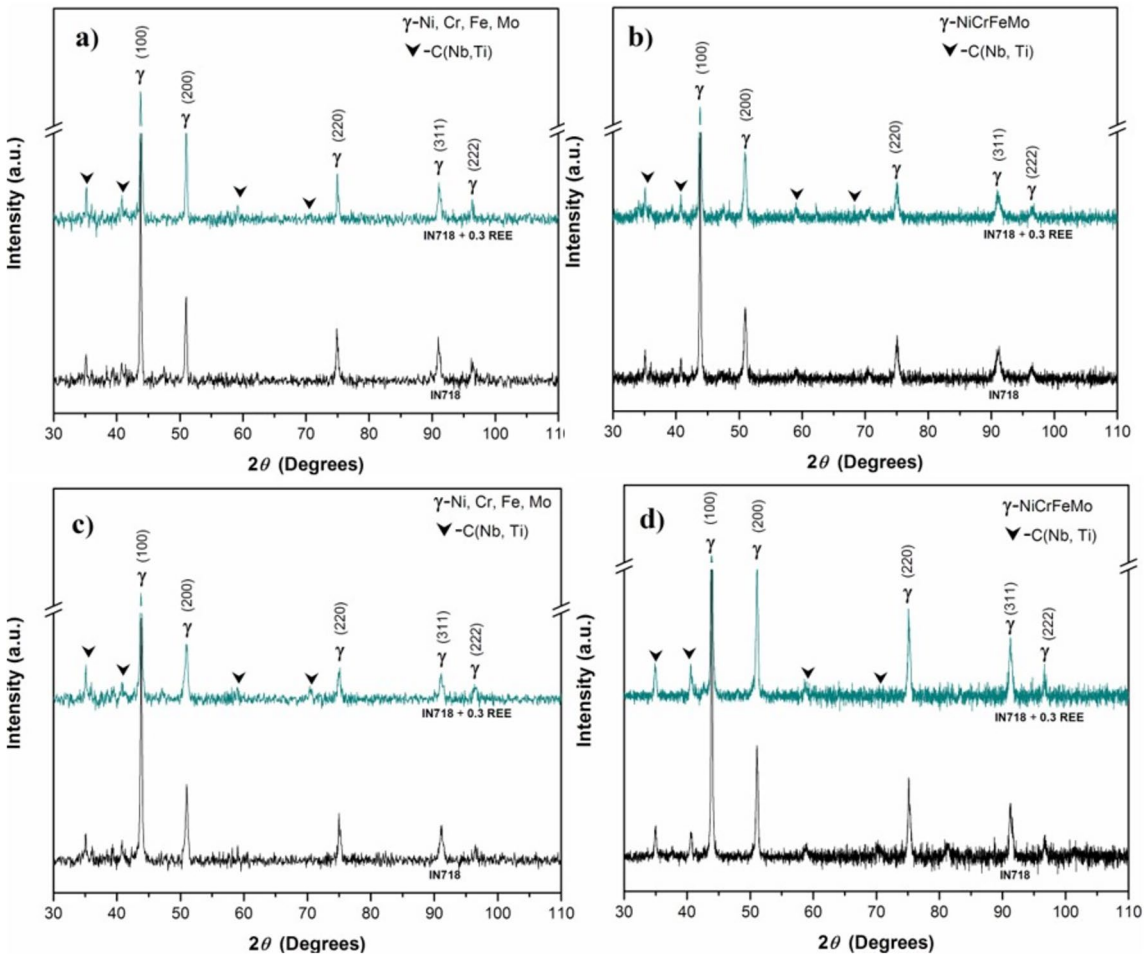

Fig. 3 XRD patterns corresponding to IN718 alloy and alloy with 0.3 REE (wt.%) after conventional (**a**) and HIP (**b**) sintering and aging treatment (**c** and **d**, respectively).

authors [13], which reported that the volume fraction of γ′ is approximately four times lower than γ″ precipitates in IN718 aged alloys [6, 7].

Table 1 shows the parameters of ϕ, L, and h, diameter, length and thickness, respectively, for the precipitate phases in the IN718 alloy and the alloy with additions of 0.3 REE (wt. %). The minor size observed in the precipitates, concerning the reported by Slama et al. [7], is highly associated with the REE addition in IN718 alloy; it has been reported that the use of REE additions in metal matrix materials such as Ni-Co alloys, induces thermal stability because its low thermal conductivity and high thermal expansion as principal characteristics [17].

On the other hand, the NBED pattern shows principal reflection spots, which correspond to the γ matrix, and the minor intensity reflection spots correspond to γ′ and γ″ precipitates. The presence of faint rings in the center in the diffraction pattern is attributed to the nanosized grains obtained during the MA process.

Figure 6 shows the HV values obtained from IN718 alloy and those with additions of 0.1, 0.2 and 0.3 REE (wt. %) after CS and HIP sintering and solution and aging treatment. The results show that HIP sintered samples present higher hardness values than CS ones. In both sintering routes, it is observed that the solution heat treatment increases the hardness, and the aging treatment considerably raises the hardness values concerning the solubilized condition due to the forming γ′ and γ″ nanoprecipitates. Furthermore, the addition of REE slightly favors the increase in microhardness. However, the process of sintering by HIP has a more notable effect, which could be attributed to the high numeric density of dispersed oxides and carbides acting as reinforcing phases. In addition, the solid solution strengthening is generated by REE addition and dissolution of Nb, Ti and Mo rich phases, high homogeneity, and a dense microstructure promotes the formation of an ultra-fine microstructure with isotropic properties [4, 18].

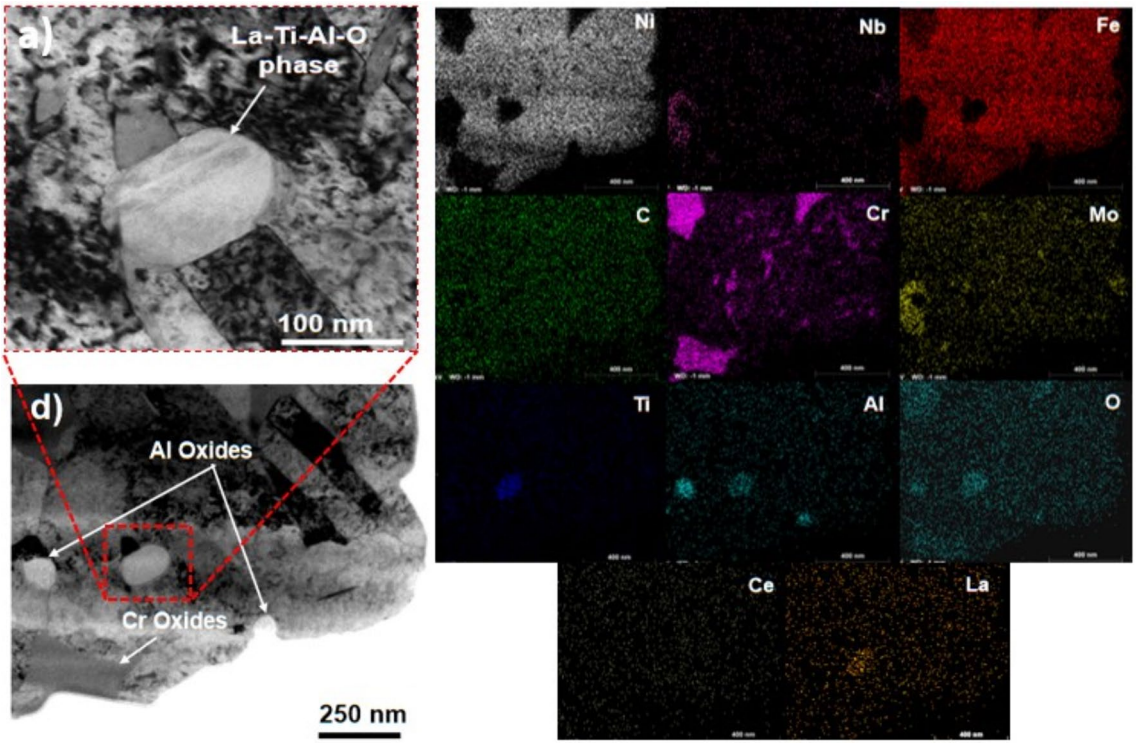

Fig. 4 STEM-BF micrographs and EDS-mapping of IN718 alloy with 0.3 REE (wt.%) after HIP sintering and aging treatment.

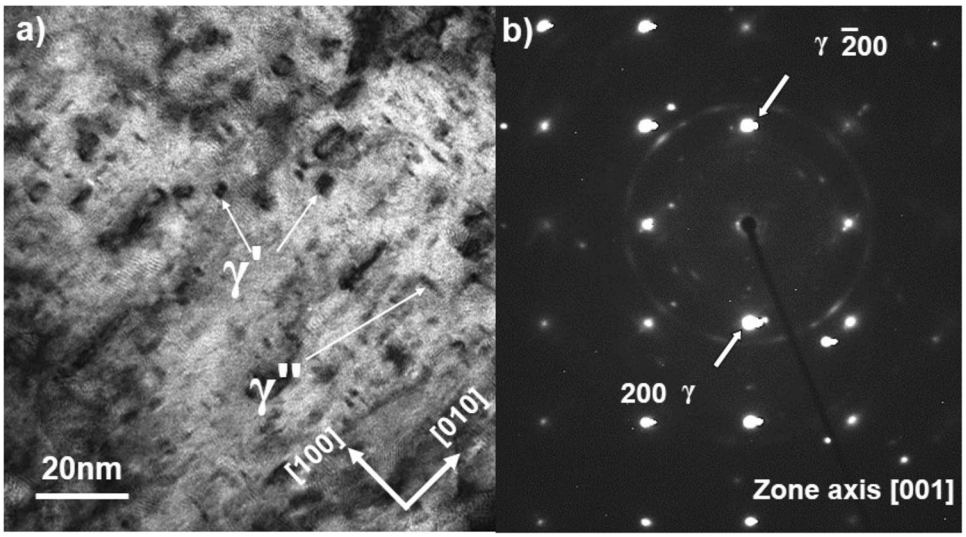

Fig. 5 BF-TEM micrograph (**a**) and the TEM-NBED pattern (**b**) corresponding to the IN718 alloy with 0.3 RE (wt.%) after HIP sintering and aging treatment.

Table 1. Parameters of ϕ, L, and h, diameter, length and thickness, respectively, for the precipitate phases in the IN718 alloy and the alloy with additions of 0.3 REE (wt. %)

HIP Aged Superalloys	Precipitates phases		
	γ'' (Ni_3Nb)		γ' Ni_3(Ti, Al)
IN718	L = 40–85 nm	h = 6–15 nm	ϕ = 38–50 nm
IN718 + 0.3 REE (wt%)	L = 3–7 nm	h = 1.5–2.5 nm	ϕ = 5–22 nm

Conclusion

The findings indicate that IN718 alloy benefits from a range of strengthening mechanisms following the incorporation of REE. These mechanisms encompass solid solution strengthening, the dispersion of second-phase particles, and precipitation hardening, all achieved through the

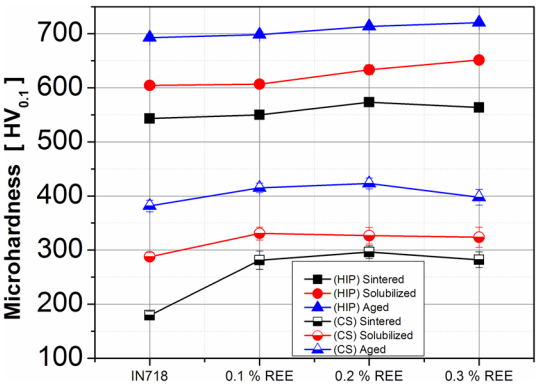

Fig. 6 Vickers microhardness values obtained from IN718 alloy and those with additions of 0.1, 0.2 and 0.3 REE (wt.%) after conventional and HIP sintering and solution and aging treatments.

various stages of the powder metallurgy process, sintering, and subsequent heat treatments.

The HIP sintering process substantially enhances hardness compared to CS sintering, approximately doubling the hardness value. This improvement can be attributed to several factors, including the high numerical density of dispersed oxides and carbides that serve as reinforcing agents. Additionally, introducing REE and dissolving elements in the phases rich in Nb, Ti, and Mo contribute to solid solution strengthening. The process also ensures high homogeneity and a dense microstructure, facilitating the development of an ultra-fine microstructure with isotropic properties.

On the other hand, for REE additions, the La present affinity with Ti, Al, and O to form new phases that contribute to the strengthening mechanism by dispersion of second-phase particles. The REE induces thermal stability in the alloy due to the diffusion of those elements into the matrix to create a solid solution. Furthermore, such adding contributes to the minor size of γ′ and γ″ precipitates due to high thermal stability in the system.

Acknowledgments The technical assistance of K. Campos-Venegas and C. C. Leyva-Porras for SEM characterization, R. Ochoa-Gamboa and C. Ornelas for TEM characterizations, E. Guerrero-Lestarjette for XRD characterization and L. D. Laguna-Zubía, D. Villalobos-Gonzalez, P. A. Guerrero-Seañez, M. A. Rascón-Sánchez for the collaboration in experimental work is greatly appreciated. The first author, HMMP CVU 344431, would like to thank CONAHCYT for the postdoctoral scholarship.

References

1. N. Nayan, N.P. Gurao, S.V.S. Narayana-Murty, A.K. Jha, B. Pant, K.M. George, Microstructure and micro-texture evolution during large strain deformation of Inconel alloy IN718. Mater Charact. **110**, 236–241 (2015). https://doi.org/10.1016/j.matchar.2015.10.027
2. E. Bassini, V. Vola, M. Lorusso, R. Ghisleni, M. Lombardi, S. Biamino, D. Ugues, G. Vallillo, B. Picqué, Net shape HIPping of Ni-superalloy: Study of the interface between the capsule and the alloy. Mater. Sci. Eng. A. **695**, 55–65 (2017). https://doi.org/10.1016/j.msea.2017.04.016
3. M.-S. Chen, Z.-H. Zou, Y.C. Lin, H.-B. Li, G.-Q. Wang, Y.-Y. Ma, Microstructural evolution and grain refinement mechanisms of a Ni-based superalloy during a two-stage annealing treatment. Mater Charact. **151**, 445–456 (2019). https://doi.org/10.1016/j.matchar.2019.03.037
4. G.A. Rao, M. Kumar, M. Srinivas, D.S. Sarma, Effect of standard heat treatment on the microstructure and mechanical properties of hot isostatically pressed superalloy inconel 718. Mater. Sci. Eng. A. **355**, 114–125 (2003). https://doi.org/10.1016/S0921-5093(03)00079-0
5. G.A. Rao, M. Srinivas, D.S. Sarma, Influence of modified processing on structure and properties of hot isostatically pressed superalloy Inconel 718. Mater. Sci. Eng. A. **418**, 282–291 (2006). https://doi.org/10.1016/j.msea.2005.11.031
6. A. Chamanfar, L. Sarrat, M. Jahazi, M. Asadi, A. Weck, A.K. Koul, Microstructural characteristics of forged and heat treated Inconel-718 disks. Mater. Des. **52**, 791–800 (2013). https://doi.org/10.1016/j.matdes.2013.06.004
7. C. Slama, M. Abdellaoui, Structural characterization of the aged Inconel 718. J. Alloys Compd. **306**, 277–284 (2000). https://doi.org/10.1016/S0925-8388(00)00789-1
8. M. Jambor, O. Bokůvka, F. Nový, L. Trško, J. Belan, Phase transformations in nickel base superalloy inconel 718 during cyclic loading at high temperature. Prod. Eng. Arch. **15**, 15–18 (2017). https://doi.org/10.30657/pea.2017.15.04
9. I.M. Makena, M.B. Shongwe, M.M. Ramakokovhu, M.L. Lethabane, Effect of heating rate on the density, hardness and microstructural properties of spark plasma sintered Ni-Fe-Cr alloys. Proc World Congr. Eng. **2**, 1–6 (2017)
10. S. Pasebani, A.K. Dutt, J. Burns, I. Charit, R.S. Mishra, Oxide dispersion strengthened nickel based alloys via spark plasma sintering. Mater. Sci. Eng. A. **630**, 155–169 (2015). https://doi.org/10.1016/j.msea.2015.01.066
11. A.K. Chaudhari, V.B. Singh, Impact of CeO2 incorporation in electrodeposited Ni-Fe on structure and physical properties of multifunctional nanocomposites. Arab. J. Chem. **12**, 5028–5039 (2019). https://doi.org/10.1016/j.arabjc.2016.11.007
12. Yu. Li, Lu. Zheng, S. Peng, X. Li, Effect of Al/Ti ratio on γ′ and oxide dispersion strengthening in Ni-based ODS superalloys. Mater. Sci. Eng. A. **845**, 143240 (2022). https://doi.org/10.1016/j.msea.2022.143240
13. S.M. Seyyed-Aghamiri, H.R. Shahverdi, S. Ukai, N. Oono, K. Taya, S. Miura, S. Hayashi, T. Okuda, Microstructural characterization of a new mechanically alloyed Ni-base ODS superalloy powder. Mater Charact. **100**, 135–142 (2015). https://doi.org/10.1016/j.matchar.2014.12.008
14. e.g.,A. Luis, A. Bedolla-Jacuinde, F.V. Guerra et al., Influence of rare earth additions to an inconel 718 alloy. MRS Adv. **5**, 3035–3043 (2020). https://doi.org/10.1557/adv.2020.387
15. W. Jasinski, P. Zawada, Stability of superalloys doped with rare earth elements. Key Eng. Mater. **586**, 141–145 (2013). https://doi.org/10.4028/www.scientific.net/KEM.586.141
16. G.A. Rao, K. Satyaprasad, M. Kumar, M. Srinivas, D.S. Sarma, Characterization of hot isostatically pressed nickel base superalloy inconel 718. Mater. Sci. Technol. **19**(3), 313–321 (2003). https://doi.org/10.1179/026708303225010605
17. M. Shrivastava, V.K.W. Grips, K.S. Rajam, Electrodeposition of Ni–Co composites containing nano-CeO2 and their structure, properties. Appl. Surf. Sci. **257**, 717–722 (2010). https://doi.org/10.1016/j.apsusc.2010.07.046

18. H.V. Atkinson, B.A. Riknson, *Hot isostatic processing*, 1st edn (Bristol Adam Hilger, Philadelphia, 1991)